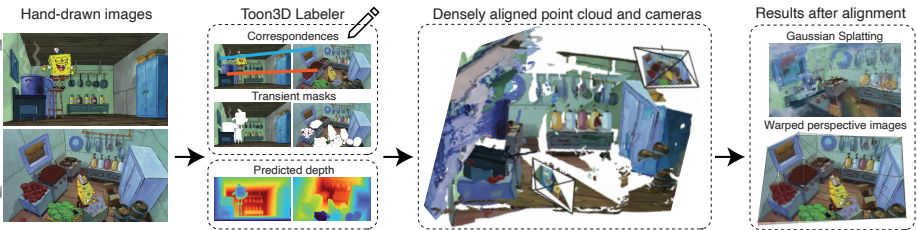


# Toon3D: Seeing Cartoons from a New Perspective

Ethan Weber<sup>\*2</sup>, Riley Peterlinz<sup>\*2</sup>, Rohan Mathur<sup>2</sup>,  
Frederik Warburg<sup>1</sup>, Alexei A. Efros<sup>2</sup>, and Angjoo Kanazawa<sup>2</sup>

<sup>1</sup>Teton.ai    <sup>2</sup>UC Berkeley



**Fig. 1: Reconstructing geometrically inconsistent scenes.** Toon3D takes a set of geometrically inconsistent images with correspondences and predicted depth maps and creates a consistent 3D model. This is achieved by warping the images in 2D and solving for camera parameters via aligning backprojected point clouds. The images are warped to fit a perspective projection. With Toon3D, we can visualize cartoons from novel views and analyze geometrical inconsistencies in the drawings.

**Abstract.** In this work, we recover the underlying 3D structure of non-geometrically consistent scenes. We focus our analysis on hand-drawn images from cartoons and anime. Many cartoons are created by artists without a 3D rendering engine, which means that any new image of a scene is hand-drawn. The hand-drawn images are usually faithful representations of the world, but only in a qualitative sense, since it is difficult for humans to draw multiple perspectives of an object or scene 3D consistently. Nevertheless, people can easily perceive 3D scenes from inconsistent inputs! In this work, we correct for 2D drawing inconsistencies to recover a plausible 3D structure such that the newly warped drawings are consistent with each other. Our pipeline consists of a user-friendly annotation tool, camera pose estimation, and image deformation to recover a dense structure. Our method warps images to obey a perspective camera model, enabling our aligned results to be plugged into novel-view synthesis reconstruction methods to experience cartoons from viewpoints never drawn before. Our project page is <https://toon3d.studio/>.

**Keywords:** 3D Reconstruction · Non-geometric · Deformation

## 1 Introduction

Humans typically have little trouble inferring the relative camera poses and 3D structure from hand-drawn cartoons. However, current structure-from-motion

<sup>\*</sup> Equal contribution

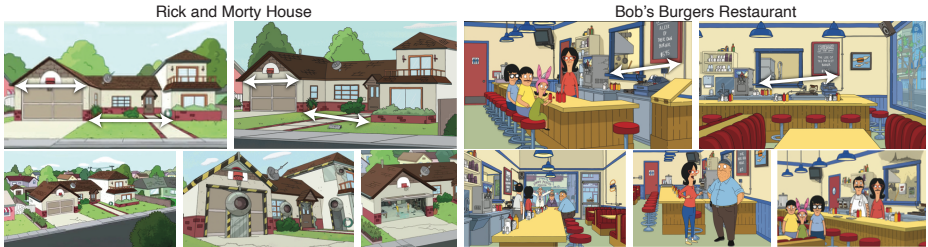


**Fig. 2: Geometrical inconsistencies in cartoons.** Are these white arrows consistent? It is incredibly difficult to tell as a human, but COLMAP and SfM pipelines fail on these images, even with our hand-labeled correspondences.

(SfM) pipelines fail to reconstruct these scenes because (1) the images are not geometrically consistent, (2) the images do not obey physically plausible camera models, and (3) the scenes are typically only drawn from a sparse set of views as shown in Fig. 2. In this work, we overcome these challenges by proposing a non-rigid piecewise-rigid deformable optimization framework (see Fig. 1) that recovers camera poses and dense structure from non-geometrically consistent images. We reconstruct a plausible 3D structure for hand-drawn scenes, and the deformed input images obey a perspective camera model.

Our pipeline consists of three main steps as follows: sparse alignment, dense alignment, and 3D Gaussian refinement. *1) Sparse alignment.* Our pipeline takes a set of correspondences as input, which we backproject into 3D using the depth from a monodepth network [19]. We align these sparse correspondences in 3D to coarsely estimate the camera intrinsic and extrinsic parameters. *2) Dense alignment.* Starting from this camera configuration, we initialize a 3D mesh at the sparse correspondences and deform its vertices until achieving near-perfect alignment at the 3D correspondences. We regularize our warps with 2D and 3D rigidity losses to prevent degenerate solutions. Finally, we can use our aligned mesh with barycentric interpolation to densely warp the RGB images in 2D and the depth map in 3D. *3) Gaussian refinement.* We use our densely aligned point cloud to initialize 3D Gaussian Splatting [20] to enable a more immersive visual experience than point clouds or meshes.

We also propose the Toon3D Labeler which is a user-friendly annotation tool, where a user can label point correspondences between images while segmenting transient objects. The Toon3D Labeler is a hosted website with no installation, so anyone can get up and running with it easily. We intentionally highlight Toon3D Labeler as a contribution of our paper because artists work with cartoon drawings regularly, and this tool fits nicely into a human-in-the-loop framework for recovering 3D from these drawings. Our recovered 3D model may help artists draw novel viewpoints. We use our labeler to label 12 scenes from popular cartoons and anime, such as Sponge Bob (Fig. 1) and Spirited Away, and we release these as the Toon3D Dataset.

To the best of our knowledge, we are the first to present a pipeline for reconstructing cartoon or hand-drawn scenes. Our pipeline yields reliable camera poses, whereas COLMAP [28] fails to estimate camera poses (even with human-annotated correspondences) due to geometrical inconsistencies. Furthermore, the 2D image warpings of the original images enable us to better reconstruct the full 3D geometry, while also revealing geometrical inconsistencies in the drawings.

We evaluate our pipeline on 12 popular scenes (10 cartoon TV shows, 1 movie) to highlight the effectiveness of our pipeline in obtaining good camera poses and reconstructions. We show reconstructions of our recovered 3D point clouds and renders of our estimated 3D Gaussian Splatting [20] representation. We evaluate our proposed alignment steps and losses qualitatively and quantitatively. We demonstrate that our warps can highlight geometric inconsistencies in hand-drawn images. To further validate the quality of our estimated poses, we show that we can obtain the 3D geometry of Airbnb rooms with sparse views. Finally, we show that Toon3D is also useful for reconstructing the 3D geometry from paintings depicting the same landmark from different views.

Toon3D is a step toward achieving a qualitative 3D understanding of cartoons. Humans can perceive scenes that are not necessarily 3D consistent but current algorithms cannot process such imagery due to non-perspective or non-consistent drawings. We validate our pipeline and will release all data, code, and tools for easily processing any cartoon. We hope our contribution serves as a useful framework to build upon for 3D cartoon understanding. Please see our project page <https://toon3d.studio/> for additional video results.

## 2 Related work

**Multi-view geometry estimation.** Structure-from-Motion (SfM) [12,30] takes in images, detects and matches correspondences, and solves for camera parameters. COLMAP [28] is a popular SfM pipeline, but it fails for wide baseline images (few correspondences), images with a lot of moving objects, or geometric inconsistencies typically present in cartoons. Improvements in keypoint detection [9,10], matching [27,32] and optimizations [35] have been proposed to better handle wide baselines [37] and be robust to transient objects [3], however, we are the first to adapt an SfM method to non-geometrical scenes. Our pipeline allows the user to annotate reliable correspondences and transient regions, while our novel per image warping handles the non-geometrical deformations often seen in cartoons.

After recovering camera parameters, multi-view stereo (MVS) methods, such as NeRF [22] or Gaussian Splatting [20], can be used to create dense 3D reconstructions. Most MVS methods degrade when the scene is only seen from a sparse set of views. Many works [23,39–41] incorporate priors to reduce blurry artifacts. In our pipeline, we use monodepth prior [19] to obtain a point cloud that we use to initialize our Gaussian Splatting representation.

**Reconstructing image collections.** Facade [7], a seminal early work in image-based modeling and rendering, used a set of photographs of an architectural



**Fig. 3: Toon3D Labeler.** Here are some screenshots from our Toon3D Labeler. We can label points and masks, and we can visualize any set of these and the depth map. This is a general labeling tool but especially useful for obtaining the inputs required for Toon3D.

scene to recover a textured 3D model using structure-from-motion with human-specified volumetric constraints. Phototourism [30] and Building Rome in a Day [1] pioneered the use of large online photo collections for 3D reconstruction. Object-centric methods like CMR [17, 18] recover 3D models of animals which can explain each image with a deformation. For non-rigid dynamic scenes, there exist methods like Nerfies [24] which explain small variations in a video via a 3D model with a time-conditioned warp field. With methods that require deformation, techniques such as ARAP [31] are useful. Cartoons, in contrast, have multiple images depicting the same instance but are not geometrically consistent [34]. This is a different and under-explored problem setting.

**Paintings to 3D.** Most attempts at recovering 3D from drawings and paintings have focused on the single view setting, with missing 3D information provided either manually by the user or via learning. Important early user-assisted approaches for generating 3D scenes from a single painting include Tour into the Picture [14], which assumed single-point perspective, and the more general Single View Metrology [5]. Automatic Photo Popup [13] replaced the manual parts of the reconstruction process with early machine learning techniques, and was able to generalize to paintings. Aubry *et al.* [2] is a rare attempt to connect different paintings of the same scene by using a 3D model. There has also been a few attempts to recover a 3D model from a set of sketches of the same object [8, 11].

**Computer vision in TV and Film.** SfM and NeRF has been used to reconstruct and analyze sitcom TV shows: Pavlakos *et al.* [25] recover camera shot locations, 3D poses of humans, and provide gaze understanding, enabling applications such as post-production re-rendering with novel camera paths. MovieNet [15] proposes a large dataset of popular films annotated with bounding boxes, actions, and cinematic style for a holistic understanding of movies. Zhu *et al.* [43] proposes to align movies and books to obtain fine-grained descriptions of appearances of objects and characters as well as high-level semantic understanding into how characters think and reason. Additionally, some works have looked into character reconstruction for cartoon characters [4, 16, 29] but none have looked at recovering camera poses and reconstructing full 3D environments. Our work is most similar to [25], but we use hand-drawn cartoons with inconsistencies instead of real sitcom frames.

### 3 Toon3D Labeler and Dataset

We present the Toon3D Labeler and Toon3D Dataset, which consists of 12 cartoon scenes (10 TV shows, 1 movie) and 78 labeled images. Tab. 1 (left column) lists our cartoon scenes. Associated with the dataset, we highlight the Toon3D Labeler (Fig. 3), which we develop to create the dataset. The Toon3D Labeler is a hosted website with no installation, so anyone can access and use it. It fits nicely into a human-in-the-loop framework for recovering 3D from these drawings.

#### 3.1 Data processing and labeling

**Preprocessing.** We collect a set of  $N$  images denoted by  $I = \{I_i|I_1, \dots, I_N\}$ . Each scene typically has  $N \leq 10$  images with wide baselines. We preprocess these images by running a monocular depth network to obtain predicted depths  $D = \{D_i|I_1, \dots, I_N\}$ . We normalize our depth maps by dividing it by the maximum value across all depth maps. We use Marigold [19] for the depth prediction. We also run Segment Anything (SAM) [21] to get a set of masks per image.

**Labeling.** We create an annotation tool, Toon3D Labeler, designed to take the preprocessed data and display it in our custom web viewer for labeling points and selecting SAM masks as transient regions to discard. We also have the ability to visualize the depth map in the viewer to make sure to avoid clicking points directly on depth discontinuities. To select SAM mask, the user simply hovers over a region, the mask will be highlighted, and it can be toggled on and off to discard those transient pixels. Also, our annotation tool is useful for scenes where COLMAP fails and one wants hand-labeled correspondences *e.g.* Sec. 5.4.

At the end of labeling, we obtain a set of pixel correspondences  $\mathcal{X} = \{x_{i,c}\}$  where  $i$  is the image index and  $c$  is the correspondence index. We also have a valid correspondences mask  $m_{i,c} = \{0, 1\}$ . When  $m_{i,c} = 0$ , the correspondence is not visible from that viewpoint. We denote the predicted depth of the correspondences with  $d_{i,c} = D_i(x_{i,c})$ .

## 4 Method

Our method, Toon3D, consumes point correspondences and mask annotations and then performs the steps of sparse alignment followed by dense alignment to output camera poses, a 3D point cloud, and warped images that obey a perspective camera model. We load this point cloud into Gaussian Splatting to create a more immersive novel-view experience and visualize the warps to highlight geometrical inconsistencies in the input images. Fig. 4 shows an overview of our framework.

### 4.1 Sparse alignment

The first step of our pipeline obtains an initial set of camera poses. Simply using our human annotated correspondences with COLMAP fails due to the geometric inconsistencies in cartoon drawings. Instead, we propose to backproject the correspondences into 3D with a predicted depth to create a point cloud  $P_i$  and

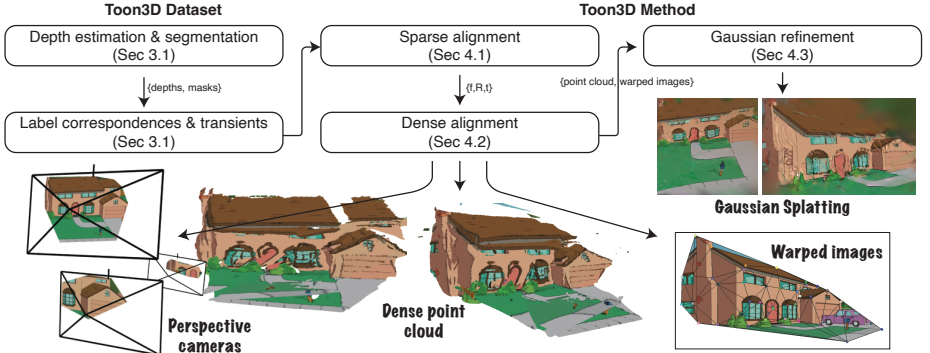


**Fig. 4: Pipeline overview.** Our framework consists of labeling images with our interactive Toon3D Labeler tool, recovering camera poses and aligning a dense point cloud, and visualizing the dense reconstruction with Gaussians to create an immersive visual experience.

solve for camera rotations  $R$ , translations  $t$ , focal length  $f$ , depth scale  $s$ , and shift  $h$  that maximize alignment. More precisely, points are backprojected as follows:

$$p(x_{i,c}) = R_i \cdot K_i^{-1} \cdot (s_i \cdot d_{i,c} + h_i). \quad (1)$$

Our main loss pulls together correspondences in 3D

$$\mathcal{L}_{3D} = \frac{1}{|\mathcal{X}|} \sum_{i=1}^N \sum_{j < i}^N \sum_{c=1}^M m_{i,c} \cdot \|p(x_{i,c}) - p(x_{j,c})\|_2^2. \quad (2)$$

In addition, we apply the following losses for regularization

$$\mathcal{L}_{scale} = \|1 - \frac{1}{N} \sum_{i=1}^N s_i\|^2, \quad \mathcal{L}_{aspect} = \sum_{i=1}^N \|1 - \frac{f_{i,x}}{f_{i,y}}\|^2, \quad \mathcal{L}_{focal} = \sum_{i=1}^N f_{i,x} + f_{i,y}, \quad (3)$$

where  $\mathcal{L}_{scale}$  encourages a scale close to 1 such that the scene does not shrink,  $\mathcal{L}_{aspect}$  balances  $f_{i,x}$  and  $f_{i,y}$  to maintain aspect ratio of the camera with the original image, and  $\mathcal{L}_{focal}$  penalizes large focal length to prefer wide-angle cameras over far away and zoomed in shots. We also have losses that penalize scales  $s_i$  and shifts  $h_i$  if they become negative with  $\mathcal{L}_{neg}(x) = \|\frac{1}{N} \sum_{i=1}^N \max(0, -x_i)\|^2$ . Our sparse alignment objective is as follows:

$$\begin{aligned} \arg \min_{R,t,f,s,h} \mathcal{J}_{sparse} = & \mathcal{L}_{3D} + \lambda_{scale} \mathcal{L}_{scale} + \lambda_{aspect} \mathcal{L}_{aspect} + \lambda_{focal} \mathcal{L}_{focal} \\ & + \lambda_{neg} (\mathcal{L}_{neg}(s) + \mathcal{L}_{neg}(h)) \end{aligned} \quad (4)$$

## 4.2 Dense alignment

With a coarse estimate of the camera poses recovered, we refine the sparse key-points and densely align the point clouds with 2D image warping and 3D depth

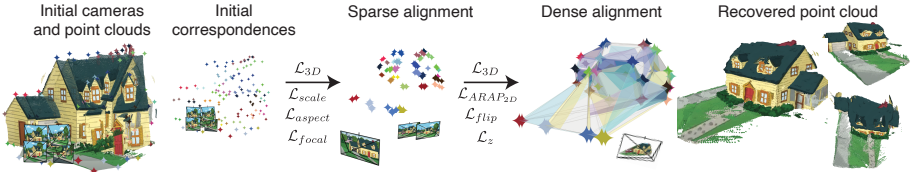


**Fig. 5: Sparse & Dense Alignment Steps.** The sparse alignment stage coarsely aligns the point clouds while optimizing for camera intrinsics and extrinsics. Dense alignment refines these estimates while also warping the images to obey a perspective camera model. After the refinement stages, we obtain a point cloud and posed images.

warping. This entails warping the images in 2D to better align the sparse correspondences and adjusting the dense depth to better align to the sparse points. To do this, we first turn each training image and predicted depth into a 3D mesh with vertices  $V \in \mathbb{R}^{M \times 3}$  and faces  $F \in \mathbb{R}^{K \times 3}$ . We then apply a piecewise-rigid deformation to this mesh, where  $V_{i,xy}$  is the initial 2D point for image  $i$  and  $V_{i,z}$  is the initial depth. We optimize the  $V$  of each image with various 2D and 3D regularizers to constrain the warps. We do this while repeating the optimization from Sec. 4.1 but now more freedom is allowed to further minimize  $\mathcal{L}_{3D}$  and find a solution, shown in Fig. 5 where the colored star points converge in dense alignment.

**Image vertices and topology.** We turn each image into vertices and faces, which represent the 2D warp and depth offset. We do this by first marking all labeled correspondences  $x_{i,c}$  as vertices. We use Delaunay triangulation to create the mesh. Selecting vertices near depth boundaries results in meshes with edges that lie on natural edges. This helps make the warps look more natural since our warping is applied to update the image color and depth with dense interpolation. See Fig. 6 for a depiction of our topology and how it looks in 3D.

**Rigidity regularizers.** We regularize the warps to prevent degenerate solutions. Our losses seek to maintain a good structure in 2D while pulling the dense 3D structure into place. We propose three main losses.  $\mathcal{L}_{ARAP_{2D}}$  [17, 31] encourages the triangles to maintain a similar orientation and spacing to their starting configuration.  $\mathcal{L}_{flip}$  penalizes if the triangle face gets too small or flips.  $\mathcal{L}_z$  encourages the warped depth to be similar to the original predicted depth. More specifically,

$$\mathcal{L}_{ARAP_{2D}} = \frac{1}{N \times |\mathcal{F}|} \sum_{i=1}^N \sum_{f \in F_i} \|V_i[f] - A_{i \rightarrow j} V'_i[f]\|^2, \quad (5)$$

$$\mathcal{L}_{flip} = \frac{1}{N \times |\mathcal{F}|} \sum_{i=1}^N \sum_{f \in F_i} \|\min(0, t_{area} - \det(V_i[f]))\|^2, \quad (6)$$

$$\mathcal{L}_z = \frac{1}{N \times |\mathcal{X}|} \sum_{i=1}^N \sum_{c=1}^M m_{i,c} \cdot \|d'_{i,c} - d_{i,c}\|, \quad (7)$$

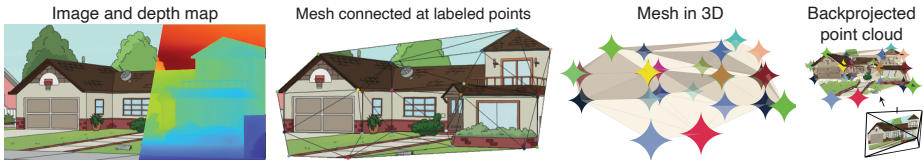


**Fig. 6: Image mesh topology.** We start with an image and predicted depth map (left). Then, we create a mesh with the 2D correspondences to define the topology (middle left). This mesh lives in 3D, where larger diamonds are closer to the camera (middle right). We can query the RGB and depth map to update the dense 3D point cloud using barycentric interpolation on this mesh.

where  $A_{a \rightarrow b} \in \mathbb{R}^{2 \times 3}$  is the best fit 2D rigid transformation in the image plane that transforms vertices from face  $a$  to face  $b$ ,  $V_i[f] \in \mathbb{R}^{3 \times 3}$  is the vertices indexed at face  $f$ ,  $t_{area}$  is the minimum area a face can be, and  $\det$  gives the signed face area. We set  $t_{area}$  to 10% of the original face area. Our dense alignment objective is as follows:

$$\arg \min_{R, t, f, s, h, V} \mathcal{J}_{\text{dense}} = \mathcal{J}_{\text{sparse}} + \lambda_{ARAP_{2D}} \mathcal{L}_{ARAP_{2D}} + \lambda_{flip} \mathcal{L}_{flip} + \lambda_z \mathcal{L}_z \quad (8)$$

**Dense interpolation.** Finally, we use barycentric interpolation to warp the RGB and depth maps according to our deformed vertices  $V'$ . We warp the RGB image with barycentric interpolation according to the original vertices  $V$  and the deformed mesh  $V'$ . Similarly, we compute a depth offset and apply it to the original depth images  $d_i$  to obtain  $d'_i$ . The resulting output is an image and depth map that obey the perspective camera model as well as the global 3D geometry.

### 4.3 Gaussian refinement

At this point, we have aligned depth maps which are backprojected into a combined 3D point cloud. We could visualize the point cloud as-is, but we find that Gaussian Splatting can create a more immersive experience. Gaussian Splatting [20] is typically initialized by a sparse point cloud from COLMAP, but instead, we initialize it with our dense point cloud. We add a few sparse-view regularizers including the ranking loss from [38] (to reconstruct scenes to be consistent with the predicted depth) and a total variation [42] loss in novel views interpolated between pairs of training views.

## 5 Experiments

### 5.1 Cartoon reconstruction

In Fig. 7 we show the results from our pipeline on multiple popular cartoon scenes. In the left column, we show the point cloud and some of the posed



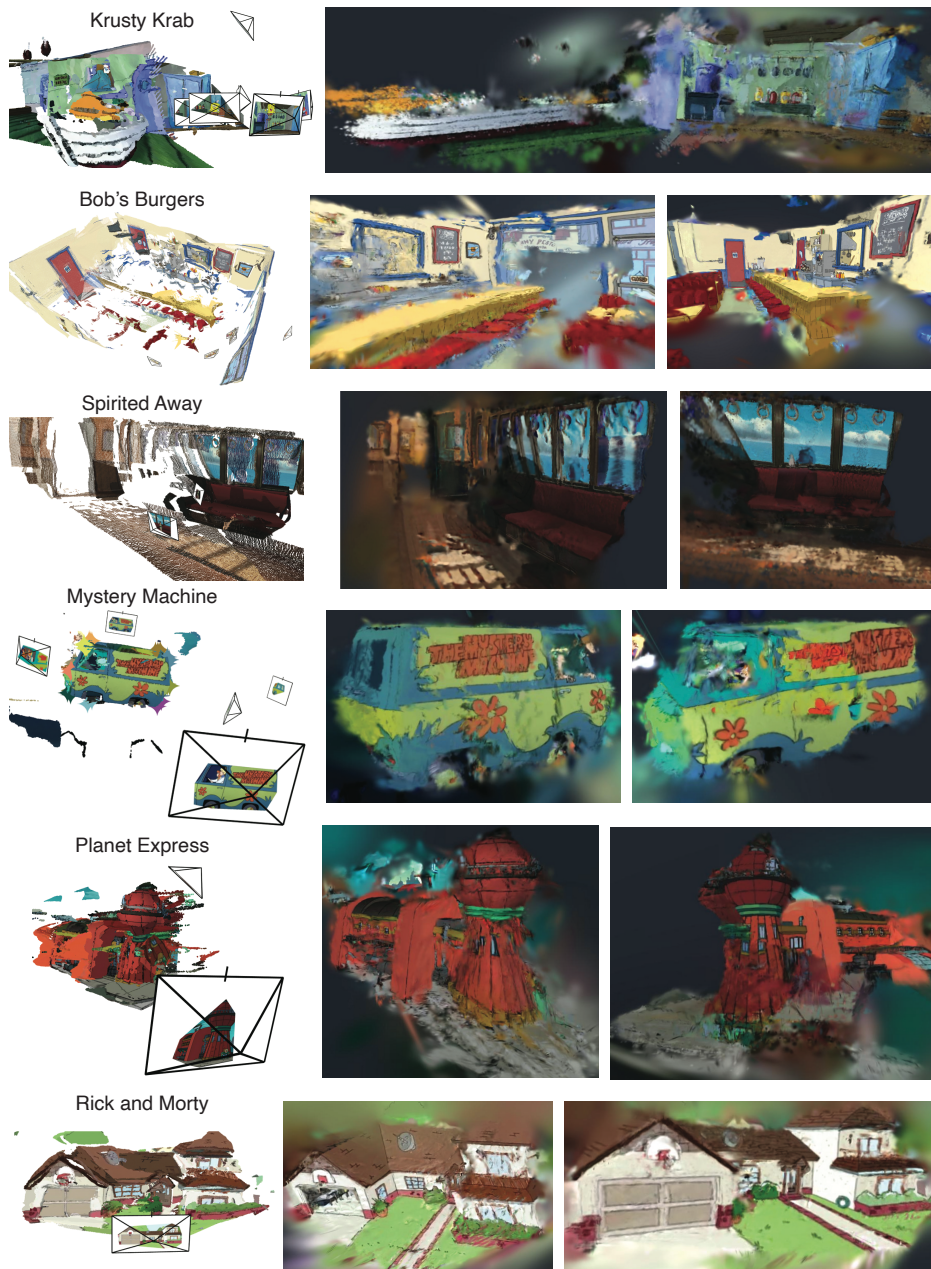


**Fig. 7: Our 3D reconstructions of cartoons.** We recover camera intrinsics and poses, reconstruct a densely aligned point cloud, and optimize the result with Gaussian Splatting to create a more immersive view. For the Krusty Krab SpongeBob scene (top), we label point correspondences between walls to reconstruct two rooms together.



**Fig. 8: Visualizing inconsistencies.** We show the most inconsistent regions in a few images from different scenes by overlaying the original image (left) on top of the warped image (right) to construct a difference image (middle). More blurry regions indicate where the images warped more to achieve 3D perspective consistency.

images found after the dense alignment stage. We have removed the labeled transient regions from the final point clouds and do not train on these regions during Gaussian refinement. The remaining columns show rendered novel views after the Gaussian refinement stage. We encourage the reader to see our project page for video results. From start to completion, our method takes on the order of minutes. Finding a few images of a cartoon scene and labeling points is quick due to the web-based viewer (Fig. 3), and running our camera alignment and warping takes approximately 1 minute on an NVIDIA RTX A5000. Running Gaussian Splatting with the Nerfstudio [33] implementation and our additional losses takes  $\sim 3$  minutes, where we train for just 2K iterations to obtain sharp results.

## 5.2 Visualizing inconsistencies

One unique aspect of Toon3D is that we keep the original images around rather than discarding them. They are warped in 2D to obey the global 3D geometry and a perspective camera model. In Fig. 8 we show where the images deform the most to create a unified consistent 3D structure. This is fundamentally different than alternative sparse-view generative methods, *e.g.* Dreambooth3D [26] which

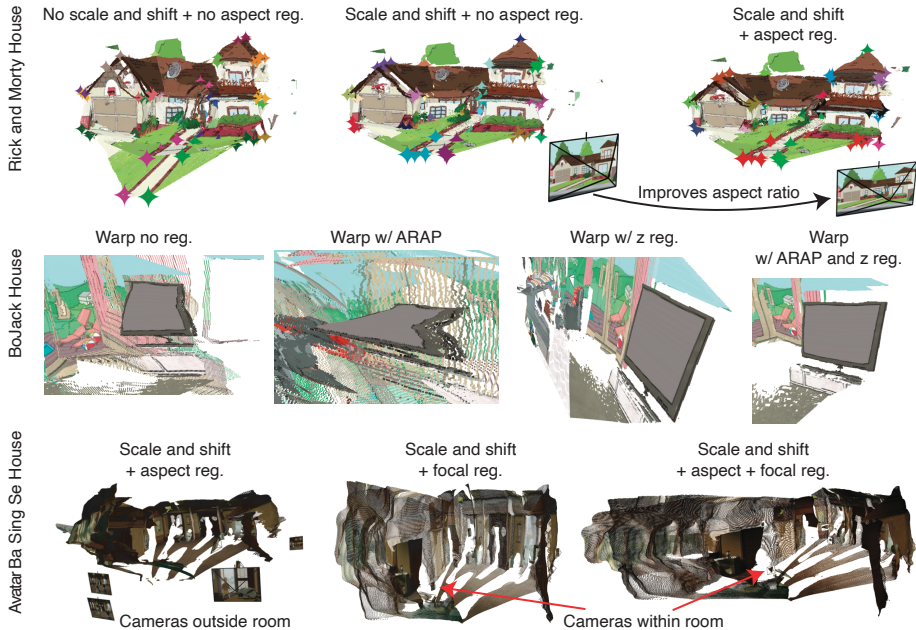


**Fig. 9: 3D alignment ablations.** Row 1 (Rick and Morty House) shows regularization’s impact on scene shaping. Optimized shift and scale parameters can adjust point clouds to better align at correspondences. This is evident as the starred points converge. The aspect regularization keeps the optimized image close to its original aspect ratio. Row 2 (BoJack Horseman House) explores the effects of different warp regularizers ( $\mathcal{L}_{ARAP_{2D}}$  and  $\mathcal{L}_z$ ) on scene warping. Without any regularization, warping distorts scene geometry. ARAP alone results in poor 3D warps due to inaccurate depth.  $z$  regularization alone limits scene movement, maintaining rigid structures close to the original depth map. Using both strikes a good balance between correctly positioning geometry and preserving structural integrity. Finally, Row 3 (Avatar House) highlights how focal regularization keeps cameras inside the building room rather than outside and zoomed in.

fine-tunes on a collection of images and then hallucinates a scene. Having access to such warp field is useful in artists workflows and might help us understand how humans perceive 3D from inconsistent 2D drawings. Additionally, it provides insights into the artistic techniques used to convey 3D or to emphasize regions in drawings without strictly adhering to physical laws.

### 5.3 3D alignment ablations

In this section, we experiment with different degrees of freedom during optimization and with different regularizations turned on during optimization. We show qualitative results in Fig. 9 and quantitative results in Tab. 1.

**Table 1: Quantitative ablations.** Here we compare various regularizers for our method. We report  $\mathcal{L}_{3D}$  on 5 correspondence points that we randomly remove from every labeled image. See Sec. 5.3 for details on the ablation names.  $W(A/Z)$  is our method with all camera parameters freely optimized and using all proposed losses. In this table, we multiply  $\mathcal{L}_{3D}$  by 100 for better readability.

| Scene            | C    | C(S) | C(S/A) | C(S/F) | C(S/A/F) | W    | W(A) | W(Z) | W(A/Z)      |
|------------------|------|------|--------|--------|----------|------|------|------|-------------|
| Avatar House     | 4.39 | 6.22 | 5.47   | 6.40   | 5.50     | 8.79 | 7.00 | 4.50 | 3.38        |
| Bob’s Burgers    | 4.14 | 3.77 | 3.80   | 3.78   | 3.81     | 3.56 | 4.58 | 4.00 | 3.86        |
| BoJack Room      | 13.4 | 21.2 | 33.8   | 20.6   | 34.7     | 16.1 | 15.3 | 12.4 | 11.6        |
| Fam. Guy Dining  | 2.72 | 2.52 | 2.80   | 2.54   | 2.81     | 4.84 | 4.90 | 2.45 | 2.50        |
| Fam. Guy House   | 3.54 | 3.92 | 3.18   | 3.99   | 3.21     | 3.51 | 3.53 | 2.93 | 2.86        |
| Krusty Krab      | 20.1 | 10.3 | 8.47   | 10.6   | 8.69     | 14.9 | 13.9 | 9.38 | 7.73        |
| Magic School Bus | 3.21 | 2.46 | 2.54   | 2.45   | 2.55     | 3.48 | 3.15 | 2.60 | 2.25        |
| Mystery Machine  | 9.99 | 18.1 | 17.0   | 17.7   | 16.3     | 12.4 | 12.7 | 10.6 | 10.8        |
| Planet Express   | 4.42 | 3.43 | 3.15   | 3.45   | 3.17     | 3.72 | 3.53 | 4.14 | 3.54        |
| Simpsons House   | 1.04 | 1.03 | 1.02   | 1.04   | 1.03     | 0.91 | 1.17 | 0.70 | 0.42        |
| Rick and Morty   | 0.90 | 0.78 | 0.77   | 0.79   | 0.78     | 2.31 | 2.51 | 0.64 | 0.53        |
| Spirited Away    | 8.01 | 9.37 | 6.31   | 9.41   | 6.37     | 5.13 | 4.67 | 5.51 | 5.25        |
| Average          | 6.32 | 6.93 | 7.36   | 6.90   | 7.40     | 6.64 | 6.41 | 4.98 | <b>4.56</b> |

**Qualitative results.** For our default method, we have all parameters free (including scale and shift) with all regularization losses turned on. We show the qualitative trade-offs for our various losses in Fig. 9. We find that our losses help align structure while maintain an accurate aspect ratio, preventing degenerate warps, and favoring cameras inside walls rather than far away and zoomed in. Please see the caption for more details.

**Quantitative results.** Our task is most naturally evaluated qualitatively, but to be thorough, we design a simple metric to evaluate 3D consistency, with results reported in Tab. 1. We randomly select and remove 5 labeled correspondence points from each image of our 12 scenes in our Toon3D Dataset. We then run our methods with various parameters and regularizations turned on and off, indicated by letters in the top of Tab. 1. We report  $\mathcal{L}_{3D}$  on these correspondences to measure their resulting distances after withholding them from optimization.  $C$  means only camera optimization is used while  $W$  means both camera optimization and image warping is applied.  $S$  means we are optimizing scale and shift. For cameras  $C$ ,  $A$  means we regularize with  $\mathcal{L}_{aspect}$ ,  $F$  means we regularize with  $\mathcal{L}_{focal}$ . For warps  $W$ ,  $A$  means we regularize with  $\mathcal{L}_{ARAP_{2D}}$  and  $Z$  means  $\mathcal{L}_z$  is used. Our proposed method uses all regularizers  $W(A/Z)$  and achieves the best results averaged over all the scenes.

## 5.4 Sparse-view reconstruction

In this section, we reconstruct sparse photo collections from two Airbnb rooms from a listing (8 photos of a bedroom, shown in the project page, and 5 photos of

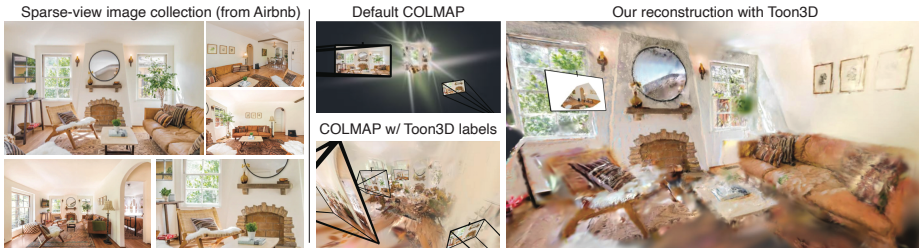


**Fig. 10: Sparse-view reconstruction.** Our pipeline can reconstruct sparse-view image collections (left). COLMAP by default registers 2 out of 5 images and fails to recover structure (middle top). Using Toon3D Labeler correspondences, we get COLMAP to work (middle bottom) but it is initialized with a very sparse point cloud and cannot recover dense details properly. Using Toon3D, we can fully reconstruct the room.

a living room, shown in Fig. 10). This task is very difficult because SfM pipelines like COLMAP fail to find enough correspondences to accurately recover all poses. Furthermore, even with accurate camera poses, the sparse-view reconstruction setting is especially hard without priors or specialized methods like RegNeRF [23] or ReconFusion [40]. We attack this sparse-view Airbnb setting with our method for two reasons: (1) to show that we can get COLMAP to work with labeled correspondences from the Toon3D Labeler and (2) to show that our end-to-end method works for real sparse photo collections, indicating applications beyond cartoons.

**Camera parameter estimation.** When running COLMAP on our Airbnb collections, default COLMAP only registers 46% of the images. This could be possibly improved with better correspondences, *e.g.* [9, 10, 36], but there is no guarantee of finding enough inlier correspondences if automated methods are used. With our Toon3D Labeler, however, we can manually label the images quickly and get COLMAP to succeed for all images. We compare the recovered COLMAP cameras with our correspondences with the cameras recovered from Toon3D. The mean relative rotation distance between corresponding pairs in our reconstructions vs. COLMAP’s is quite low at only  $8.29^\circ$ , indicating our cameras are similar to ones recovered by COLMAP with human-labeled correspondences. We do not compare translations or focal lengths due to ambiguity between the two, but we note that our camera relative rotations match COLMAP quite well, suggesting that our camera pose estimation is accurate.

**Qualitative results.** We show qualitative results for sparse-view reconstruction on real images in Fig. 10 and videos on the project page.

## 5.5 Reconstructing paintings

Our pipeline can also reconstruct paintings. In Fig. 11, we show that Toon3D can reconstruct The Trevi Fountain. We find paintings from The Oxford Dataset [6]. Our method has an advantage over automated methods like COLMAP which

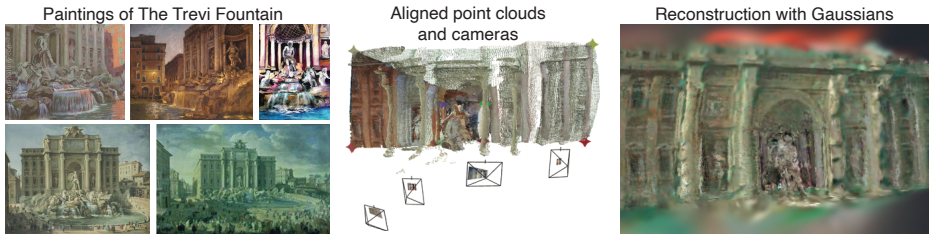


**Fig. 11: Reconstructing paintings with Toon3D.** Our method enables reconstructing paintings. On the left, we show a few paintings of The Trevi Fountain. In the middle, we show the recovered point cloud and cameras (with warped and cropped images). On the right, we densify the point cloud with Gaussian Splatting.

rely on perspective geometry and photometric consistency. Our method, alternatively, uses provided correspondences and predicted depth and then warps images into perspective images and obtains a consolidated 3D model. This enables Toon3D to work on paintings as well.

## 6 Conclusion

Our pipeline takes human-labeled correspondences and predicted depth maps as input. If either the labels are inaccurate or the predicted depth maps fail, our method will produce less accurate results. We cannot use automatic correspondence methods due to sensitivity towards outliers, so we design a user-friendly Toon3D Labeler which will be hosted online with no user installation required. This will help anyone quickly get started with labeling cartoon images and obtain a 3D model in minutes. Incorporating diffusion priors or data-driven methods to reconstruct cartoons in an end-to-end fashion could be an interesting avenue for future work. We instead present a method that relies on predicted depth and sparse correspondences to optimize cameras and non-rigid deformations such that our posed images obey perspective projection models. Finally, we encourage that our method should be used ethically and responsibly when creating content for visual media.

## Acknowledgements

This project is supported in part by IARPA DOI/IBC 140D0423C0035. The views and conclusions contained herein are those of the authors and do not represent the official policies or endorsements of IARPA, DOI/IBC, of the U.S. Government. We would like to thank Qianqian Wang, Justin Kerr, Brent Yi, David McAllister, Matthew Tancik, Evonne Ng, Anjali Thakrar, Christian Foley, Abhishek Kar, Georgios Pavlakos, the Nerfstudio team, and the KAIR lab for discussions, feedback, and technical support. We also thank Ian Mitchell and Roland Jose for helping to label points.

## Appendix

### 6.1 Video

A narrated video is available on our project page <https://toon3d.studio/>. This video contains an overview of the paper and video results. It is complementary to our paper, which is composed of screen-captured and rendered frames. Our video results are more immersive than what 2D figures can convey.

### 6.2 Toon3D Dataset

We choose to use cartoon scenes that are hand-drawn rather than using animated scenes that are rendered or based on an underlying 3D model. We select a variety of cartoons based on popularity. Table 2 shows our datasets and relevant annotation info, including how many images we use to create each scene and how many point labels are used. We use a varying number of point labels, ranging from only 46 points (Magic School Bus) to as many as 191 points (BoJack Room) in a particular scene. This range is meant to convey the robustness of our method to handle a few or many user-defined correspondences. Our Toon3D Labeler will be released so others can label scenes as they desire.

### 6.3 Sparse-view reconstruction data

We obtain sparse-view images from Airbnb from this listing: <https://www.airbnb.com/rooms/833261990707199349>. Our project page shows the two rooms and their images. The “Living room”, shown in the paper as well, has 5 images. “Bedroom 2” has 8 images. Renders of our Toon3D reconstructions are shown for both rooms on the project page.

**Table 2: Toon3D Dataset.** Here are some statistics for the Toon3D Dataset. We have  $\sim 7$  images per scene, for a total of 79 images across the 12 scenes. Each image has on average 18.3 points per image, but it varies per scene.

|                   | Num images | Num points | Average num points per image |
|-------------------|------------|------------|------------------------------|
| Avatar House      | 8          | 156        | 19.5                         |
| Bob’s Burgers     | 7          | 147        | 21.0                         |
| BoJack Room       | 12         | 191        | 15.9                         |
| Family Guy Dining | 7          | 184        | 26.3                         |
| Family Guy House  | 6          | 133        | 22.2                         |
| Krusty Krab       | 9          | 82         | 9.11                         |
| Magic School Bus  | 5          | 46         | 9.20                         |
| Mystery Machine   | 6          | 55         | 9.17                         |
| Planet Express    | 5          | 137        | 27.4                         |
| Simpsons House    | 5          | 137        | 27.4                         |
| Rick and Morty    | 4          | 99         | 24.8                         |
| Spirited Away     | 5          | 75         | 15.0                         |
| Total             | 79         | 1442       | 18.3                         |

## References

1. Agarwal, S., Snavely, N., Simon, I., Seitz, S.M., Szeliski, R.: Building rome in a day. In: 2009 IEEE 12th International Conference on Computer Vision. pp. 72–79 (2009). <https://doi.org/10.1109/ICCV.2009.5459148> 4
2. Aubry, M., Russell, B., Sivic, J.: Painting-to-3D model alignment via discriminative visual elements. *ACM Transactions on Graphics* (2013) 4
3. Bescos, B., Fàcil, J.M., Civera, J., Neira, J.: Dynaslam: Tracking, mapping, and inpainting in dynamic scenes. *IEEE Robotics and Automation Letters* **3**(4), 4076–4083 (2018) 3
4. Chen, S., Zhang, K., Shi, Y., Wang, H., Zhu, Y., Song, G., An, S., Kristjansson, J., Yang, X., Zwicker, M.: Panic-3d: Stylized single-view 3d reconstruction from portraits of anime characters. In: *CVPR* (2023) 4
5. Criminisi, A., Reid, I., Zisserman, A.: Single view metrology. *IJCV* (2000) 4
6. Crowley, E.J., Zisserman, A.: In search of art. In: *Computer Vision-ECCV 2014 Workshops: Zurich, Switzerland, September 6-7 and 12, 2014, Proceedings, Part I* 13. pp. 54–70. Springer (2015) 13
7. Debevec, P.E., Taylor, C.J., Malik, J.: Modeling and rendering architecture from photographs: A hybrid geometry-and image-based approach. In: *SIGGRAPH'96* (1996) 3
8. Delanoy, J., Aubry, M., Isola, P., Efros, A.A., Bousseau, A.: 3d sketching using multi-view deep volumetric prediction. *Proceedings of the ACM on Computer Graphics and Interactive Techniques* **1**(1), 1–22 (2018) 4
9. DeTone, D., Malisiewicz, T., Rabinovich, A.: Superpoint: Self-supervised interest point detection and description. In: *Proceedings of the IEEE conference on computer vision and pattern recognition workshops*. pp. 224–236 (2018) 3, 13
10. Dusmanu, M., Rocco, I., Pajdla, T., Pollefeys, M., Sivic, J., Torii, A., Sattler, T.: D2-net: A trainable cnn for joint detection and description of local features. *arXiv preprint arXiv:1905.03561* (2019) 3, 13
11. Guillard, B., Remelli, E., Yvernay, P., Fua, P.: Sketch2mesh: Reconstructing and editing 3d shapes from sketches. In: *Proceedings of the IEEE/CVF International Conference on Computer Vision*. pp. 13023–13032 (2021) 4
12. Hartley, R., Zisserman, A.: *Multiple view geometry in computer vision*. Cambridge university press (2003) 3
13. Hoiem, D., Efros, A.A., Hebert, M.: Automatic photo pop-up. In: *ACM SIGGRAPH 2005 Papers*, pp. 577–584 (2005) 4
14. Horry, Y., Anjyo, K.I., Arai, K.: Tour into the picture: using a spidery mesh interface to make animation from a single image. In: *Proceedings of the 24th annual conference on Computer graphics and interactive techniques*. pp. 225–232 (1997) 4
15. Huang, Q., Xiong, Y., Rao, A., Wang, J., Lin, D.: Movienet: A holistic dataset for movie understanding. In: *Computer Vision-ECCV 2020: 16th European Conference, Glasgow, UK, August 23–28, 2020, Proceedings, Part IV* 16. pp. 709–727. Springer (2020) 4
16. Jain, E., Sheikh, Y., Mahler, M., Hodgins, J.: Three-dimensional proxies for hand-drawn characters. *ACM Transactions on Graphics (ToG)* **31**(1), 1–16 (2012) 4
17. Kanazawa, A., Kovalsky, S., Basri, R., Jacobs, D.: Learning 3d deformation of animals from 2d images. In: *Computer Graphics Forum* (2016) 4, 7
18. Kanazawa, A., Tulsiani, S., Efros, A.A., Malik, J.: Learning category-specific mesh reconstruction from image collections. In: *Proceedings of the European Conference on Computer Vision (ECCV)*. pp. 371–386 (2018) 4



19. Ke, B., Obukhov, A., Huang, S., Metzger, N., Dautt, R.C., Schindler, K.: Repurposing diffusion-based image generators for monocular depth estimation (2023) **2**, **3**, **5**
20. Kerbl, B., Kopanas, G., Leimkühler, T., Drettakis, G.: 3d gaussian splatting for real-time radiance field rendering. *ACM Transactions on Graphics* **42**(4) (July 2023), <https://repo-sam.inria.fr/fungraph/3d-gaussian-splatting/> **2**, **3**, **8**
21. Kirillov, A., Mintun, E., Ravi, N., Mao, H., Rolland, C., Gustafson, L., Xiao, T., Whitehead, S., Berg, A.C., Lo, W.Y., et al.: Segment anything. *arXiv preprint arXiv:2304.02643* (2023) **5**
22. Mildenhall, B., Srinivasan, P.P., Tancik, M., Barron, J.T., Ramamoorthi, R., Ng, R.: Nerf: Representing scenes as neural radiance fields for view synthesis. *Communications of the ACM* **65**(1), 99–106 (2021) **3**
23. Niemeyer, M., Barron, J.T., Mildenhall, B., Sajjadi, M.S., Geiger, A., Radwan, N.: Regnerf: Regularizing neural radiance fields for view synthesis from sparse inputs. In: *Proceedings of the IEEE/CVF Conference on Computer Vision and Pattern Recognition*. pp. 5480–5490 (2022) **3**, **13**
24. Park, K., Sinha, U., Barron, J.T., Bouaziz, S., Goldman, D.B., Seitz, S.M., Martin-Brualla, R.: Nerfies: Deformable neural radiance fields. In: *Proceedings of the IEEE/CVF International Conference on Computer Vision*. pp. 5865–5874 (2021) **4**
25. Pavlakos\*, G., Weber\*, E., , Tancik, M., Kanazawa, A.: The one where they reconstructed 3d humans and environments in tv shows. In: *ECCV* (2022) **4**
26. Raj, A., Kaza, S., Poole, B., Niemeyer, M., Ruiz, N., Mildenhall, B., Zada, S., Aberman, K., Rubinstein, M., Barron, J., et al.: Dreambooth3d: Subject-driven text-to-3d generation. *arXiv preprint arXiv:2303.13508* (2023) **10**
27. Sarlin, P.E., DeTone, D., Malisiewicz, T., Rabinovich, A.: Superglue: Learning feature matching with graph neural networks. In: *Proceedings of the IEEE/CVF conference on computer vision and pattern recognition*. pp. 4938–4947 (2020) **3**
28. Schönberger, J.L., Frahm, J.M.: Structure-from-Motion Revisited. In: *Conference on Computer Vision and Pattern Recognition (CVPR)* (2016) **3**
29. Smith, H.J., Zheng, Q., Li, Y., Jain, S., Hodgins, J.K.: A method for animating children’s drawings of the human figure. *ACM Trans. Graph.* **42**(3) (jun 2023). <https://doi.org/10.1145/3592788>, <https://doi.org/10.1145/3592788> **4**
30. Snavely, N., Seitz, S.M., Szeliski, R.: Photo tourism: exploring photo collections in 3d. In: *ACM siggraph 2006 papers*, pp. 835–846 (2006) **3**, **4**
31. Sorkine, O., Alexa, M.: As-rigid-as-possible surface modeling. In: *Symposium on Geometry processing*. vol. 4, pp. 109–116. Citeseer (2007) **4**, **7**
32. Sun, J., Shen, Z., Wang, Y., Bao, H., Zhou, X.: Loftr: Detector-free local feature matching with transformers. In: *Proceedings of the IEEE/CVF conference on computer vision and pattern recognition*. pp. 8922–8931 (2021) **3**
33. Tancik, M., Weber, E., Ng, E., Li, R., Yi, B., Wang, T., Kristoffersen, A., Austin, J., Salahi, K., Ahuja, A., et al.: Nerfstudio: A modular framework for neural radiance field development. In: *ACM SIGGRAPH 2023 Conference Proceedings*. pp. 1–12 (2023) **10**
34. Thomas, F., Johnston, O.: The illusion of life: Disney animation. (No Title) (1995) **4**
35. Tirado-Garín, J., Warburg, F., Civera, J.: Dac: Detector-agnostic spatial covariances for deep local features. *arXiv preprint arXiv:2305.12250* (2023) **3**
36. Tyszkiewicz, M., Fua, P., Trulls, E.: Disk: Learning local features with policy gradient. *Advances in Neural Information Processing Systems* **33**, 14254–14265 (2020) **13**

37. Vallone, A., Warburg, F., Hansen, H., Hauberg, S., Civera, J.: Danish airs and grounds: A dataset for aerial-to-street-level place recognition and localization. *IEEE Robotics and Automation Letters* **7**(4), 9207–9214 (2022) [3](#)
38. Wang, G., Chen, Z., Loy, C.C., Liu, Z.: Sparsenerf: Distilling depth ranking for few-shot novel view synthesis. *arXiv preprint arXiv:2303.16196* (2023) [8](#)
39. Warburg, F., Weber, E., Tancik, M., Holynski, A., Kanazawa, A.: Nerfbusters: Removing ghostly artifacts from casually captured nerfs. *arXiv preprint arXiv:2304.10532* (2023) [3](#)
40. Wu, R., Mildenhall, B., Henzler, P., Park, K., Gao, R., Watson, D., Srinivasan, P.P., Verbin, D., Barron, J.T., Poole, B., et al.: Reconfusion: 3d reconstruction with diffusion priors. *arXiv preprint arXiv:2312.02981* (2023) [3](#), [13](#)
41. Yu, A., Ye, V., Tancik, M., Kanazawa, A.: pixelnerf: Neural radiance fields from one or few images. in 2021 *ieee*. In: *CVF Conference on Computer Vision and Pattern Recognition (CVPR)*. pp. 4576–4585 (2020) [3](#)
42. Zhou, C., Zhang, H., Shen, X., Jia, J.: Unsupervised learning of stereo matching. In: *Proceedings of the IEEE International Conference on Computer Vision*. pp. 1567–1575 (2017) [8](#)
43. Zhu, Y., Kiros, R., Zemel, R., Salakhutdinov, R., Urtasun, R., Torralba, A., Fidler, S.: Aligning books and movies: Towards story-like visual explanations by watching movies and reading books. In: *Proceedings of the IEEE international conference on computer vision*. pp. 19–27 (2015) [4](#)